DETERMINATION OF THE SEISMIC MOMENT TENSOR USING SURFACE WAVES RECORDED BY THE IMS NETWORK

Jeffrey Given[2], Ronan J. Le Bras[1], and Yu-Long Kung[2]

Comprehensive Nuclear-Test-Ban Treaty Organization[1] and Science Applications International Corporation[2]

Sponsored by the Comprehensive Nuclear-Test-Ban Treaty Organization

Contract No. 2006-1193

ABSTRACT

The Provisional Technical Secretariat (PTS) of the Comprehensive Nuclear-Test-Ban Treaty Organization (CTBTO) has been ramping-up the installation of the International Monitoring System (IMS) consisting of a network of seismic, hydroacoustic, infrasound, and radionuclide stations, since its inception in March 1997. Data from this network are automatically processed at the International Data Centre (IDC) to produce, within a few hours, a series of automatic bulletins called the Standard Event Lists (SEL1, SEL2, SEL3). After analyst review and correction as necessary the Reviewed Event Bulletin (REB) is produced. Additional information about characterization of an event as an earthquake or otherwise is also available in the Standard Event Bulletin (SEB) shortly after production of the REB. The Comprehensive Nuclear-Test-Ban Treaty (CTBT) states that the IDC will apply standard event screening criteria to each event formed. The objective of this process is to filter out events that are considered to be consistent with natural or non-nuclear man-made phenomena, leaving a reduced set of events that may require further examination. In Annex 2 of the Protocol to the Treaty, the focal mechanism is listed as possible event screening parameters.

In order to provide a focal mechanism and increase the number of elements potentially useful as screening attributes, we have in the last two years implemented two methods for moment tensor (MT) inversion. One method is based on the P body waves and the other on surface waves. Implementation of these sophisticated inversion methods has led to improvements in the calibration of the broad-band seismic network, notably quality control of the instrument responses.

We report here on the results obtained from the implementation of the surface-wave MT inversion, which uses both Rayleigh waves and Love waves. We are presenting results of the application of this inversion scheme on selected events as well as statistics showing the results of automatic use of the method. Compared to using body waves, we find that using the surface waves allows us to lower the magnitude at which it is possible to obtain an automatic MT solution.

Report Documentation Page

Form Approved
OMB No. 0704-0188

1. REPORT DATE **SEP 2008**	2. REPORT TYPE	3. DATES COVERED **00-00-2008 to 00-00-2008**

4. TITLE AND SUBTITLE **Determination of the Seismic Moment Tensor Using Surface Waves Recorded by the IMS Network**	5a. CONTRACT NUMBER 5b. GRANT NUMBER 5c. PROGRAM ELEMENT NUMBER
6. AUTHOR(S)	5d. PROJECT NUMBER 5e. TASK NUMBER 5f. WORK UNIT NUMBER
7. PERFORMING ORGANIZATION NAME(S) AND ADDRESS(ES) **Science Applications International Corporation,1710 SAIC Drive,McLean,VA,22102**	8. PERFORMING ORGANIZATION REPORT NUMBER
9. SPONSORING/MONITORING AGENCY NAME(S) AND ADDRESS(ES)	10. SPONSOR/MONITOR'S ACRONYM(S) 11. SPONSOR/MONITOR'S REPORT NUMBER(S)

12. DISTRIBUTION/AVAILABILITY STATEMENT
Approved for public release; distribution unlimited

13. SUPPLEMENTARY NOTES
Proceedings of the 30th Monitoring Research Review: Ground-Based Nuclear Explosion Monitoring Technologies, 23-25 Sep 2008, Portsmouth, VA sponsored by the National Nuclear Security Administration (NNSA) and the Air Force Research Laboratory (AFRL)

14. ABSTRACT
see report

15. SUBJECT TERMS

16. SECURITY CLASSIFICATION OF:			17. LIMITATION OF ABSTRACT	18. NUMBER OF PAGES	19a. NAME OF RESPONSIBLE PERSON
a. REPORT **unclassified**	b. ABSTRACT **unclassified**	c. THIS PAGE **unclassified**	**Same as Report (SAR)**	**7**	

OBJECTIVES

The objective of this project is to develop and integrate a Surface Waves Moment Tensor (SWMT) and moment magnitude M_w (Hanks and Kanamori, 1979) measurement in the IDC processing system to take advantage of the broad-band data sent to the CTBTO IDC. For several reasons, this additional processing item will be of use to the IDC and the monitoring community in general:

- The focal mechanism for seismic events is mentioned in Annex 2 of the Protocol to the CTBT as a potentially useful attribute for event screening.
- The additional module will be of use in the prototype processing pipeline using the IMS network that can produce a timely bulletin useful as input for agencies charged with warning the general public about impending disasters such as tsunamis.
- The IDC automatic bulletins measure the size of events using the *mb* magnitude which is known to saturate for events larger than about magnitude 6.5 (e.g., Abe, K, 1995). It is therefore useful to develop other methods of assessing the size of large events in a timely manner. For large events, the focal mechanism also provides additional information for the tsunamigenic potential of the event.
- The method may be applied to data archived at the IDC and used to check the calibration of the IMS network at low frequencies for large events whose seismic moments have been estimated by publishing agencies (Harvard Centroid Moment Tensor, [CMT]) or the United States Geological Survey (USGS).

RESEARCH ACCOMPLISHED

The fundamental mode surface waves $u_i(\omega, r_i, \theta_i)$ observed at the *i-th* receiver at point (r_i, θ_i) generated by a moment tensor source located near the origin (r = 0) has the form in the frequency domain:

$$u_i^{R,Qt}(\omega, r_i, \theta_i) = T(|M|, \omega) S^{R,Q}(\omega) P^{R,Q}(\omega, \Delta t, \Delta r_i) E_{ijk}^{R,Q}(\omega, z) M_{jk} \qquad (1)$$

$E^{R,Q}$ are the vertical (Rayleigh, R) or tangential (Love, Q) excitation functions and depend on the frequency, the source region elastic structure, and the source depth. $T(|M|,\omega)$ is the source time function, which is assumed to be a function of the scalar moment. $P^{R,Q}(\omega, \Delta t, \Delta r_i)$ represents the propagation and is a function of the specific source-receiver path. $P^{R,Q}$ includes geometric spreading and the regional variation in attenuation and phase velocity. $S^{R,Q}(\omega)$ is the response at the receiver location. Δt and Δr_i are perturbations in origin time and epicentral distance around the initial estimate of the source origin parameters. M_{jk} is the 9-element symmetric MT.

All source and path-specific parameters in Equation 1 are computed from earth models and parameters registered on a 1x1 degree grid.

The amplitude and phase spectra for the fundamental mode Rayleigh and Love waves are measured using a phase-matched filter approach to increase the signal-to-noise ratio in the measured spectra. This processing is an extension of the routine processing already used at the IDC to detect surface waves and measure M_S. The phase-matched filters are derived from a global map of phase-velocities specified with 1-degree resolution.

Two different dispersion models are available to design the phase-matched filters. One, from Stevens, et al. (2005) is based on a large tomographic inversion of Rayleigh wave phase and group velocities down to 20-s periods. The inversion directly inverts for the 1x1 degree earth structure. The resulting structure models are used to calculate both the Rayleigh and Love wave phase velocities. The second dispersion model is taken from Ekstrom, et al., (1997), which is also used in routine processing for the Global CMT project. Both models are essentially equivalent for

Rayleigh waves at periods longer than 35 s, since the CMT models were used as constraints in the tomographic inversion of Stevens, et al., 2005. For Love waves, the CMT phase velocities were derived directly from Love wave observations and are clearly more accurate. The Stevens et al. phase velocities extend down to 20 s periods, which may allow the method to be extended to smaller events.

In a routine operational setting, an initial source location and magnitude are generated by the automatic event detection system. Using the initial event parameters, a surface-wave detection and spectral measurement process determines where surface waves are observed and extracts the complex amplitude spectra corresponding to the fundamental mode Love and Rayleigh waves. A second process collects the spectra and, if there are enough observations of sufficient quality, a surface-wave MT is calculated.

The MT inversion uses an iterative least-squares method to determine the best-fitting MT and perturbation to the initial source location and origin time at a fixed depth. The inversion is repeated over the possible range of depths to determine the best fitting depth. The result is an MT solution, which can be interpreted as a combination of double-couples, and a revised hypocentral location.

The frequency range used for the inversion is selected based on the initial size of the event. The dispersion model used for the path propagation depends on the selected frequency range. For larger events, the CMT dispersion models are used and the periods are constrained to be greater than 50 s. For smaller events, the Stevens et al. Rayleigh-wave dispersion model is used and the Rayleigh-wave periods are constrained to be greater than 20 s. The current Love wave propagation phase corrections are not yet accurate enough to use the shorter-period Love waves in the inversion, and for all sources, the CMT Love-wave phase corrections are used for periods greater than 35 s. For observations at the shorter periods the source-receiver distance is further constrained.

Recent Examples of Inversion and Comparison with the CMT Results

The method has been tested on a number of recent events, including the aftershocks of the recent May 12th, 2008, Eastern Sichuan earthquake which we present in this paper. Table 1 shows the results of the inversion on eight REB events and the comparison with the CMT results when these are available, which is the case for six of them. Although not part of the CTBTO IDC automatic processing pipeline, the off-line test was completely automatic in the sense that the data selection for the inversion was part of the process, and there was no second pass where an analyst checked on the results of the inversion and modified the input as necessary. The eight events are shown on a map in Figure 1. The various focal mechanisms vary from inverse along the SW-NE fault trend delineated by the aftershocks to strike-slip along the same trend. In spite of their variety, the focal mechanisms are compatible with a compression axis perpendicular to the trend of the fault. Note that the smallest event presented in the table (orid 4755448**)** and on the figure has an Mw magnitude of 4.7. The method has the potential of routinely producing MTs for events down to a magnitude of about 4.5 when appropriate data is available.

Table 1. This table shows the results of the surface-waves MT inversion on eight REB events and the six CMT events for which a comparison was possible. The events are all aftershocks of the May 12^{h} Eastern Sichuan earthquake. The MT components are in units of 10^{17} N-m.

12 May 2008 CTBTO (4750766 Mw 5.7)				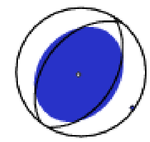
Epicenter	[32.13, 103.86]	**Mrr**	**3.71**	
Depth	20 km	**Mtt**	**-1.10**	
		Mpp	**-2.61**	
		Mrt	**-0.22**	
Time	20:08:33.6	**Mrp**	**0.26**	
		Mtp	**-0.72**	
12 May 2008 CMT (Mw 5.6)				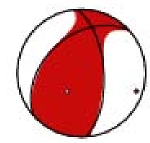
Epicenter	[32.38, 104.08]	**Mrr**	**2.31**	
Depth	28.4 km	**Mtt**	**0.46**	
		Mpp	**-2.77**	
		Mrt	**-0.68**	
Time	20:08:53.6	**Mrp**	**1.43**	
		Mtp	**-1.47**	
13 May 2008 CTBTO (4754479 Mw 5.8)				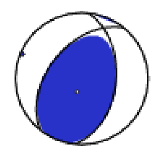
Epicenter	[31.16, 103.34]	**Mrr**	**5.88**	
Depth	20 km	**Mtt**	**-0.68**	
		Mpp	**-5.21**	
		Mrt	**-1.91**	
Time	07:07:13.0	**Mrp**	**0.58**	
		Mtp	**-2.23**	
13 May 2008 CMT (Mw 5.8)				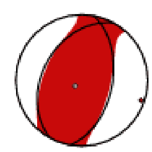
Epicenter	[30.88, 103.38]	**Mrr**	**4.85**	
Depth	14.1 km	**Mtt**	**0.34**	
		Mpp	**-5.19**	
		Mrt	**-0.26**	
Time	07:07:13.0	**Mrp**	**1.27**	
		Mtp	**-2.20**	
13 May 2008 CTBTO (4755448 Mw 4.7)				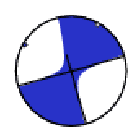
Epicenter	[32.34, 105.33]	**Mrr**	**0.008**	
Depth	20 km	**Mtt**	**0.05**	
		Mpp	**-0.06**	
		Mrt	**0.00099**	
Time	12:51:36	**Mrp**	**-0.00079**	
		Mtp	**-0.09**	
14 May 2008 CTBTO (4750217 Mw 5.5)				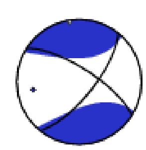
Epicenter	[31.47, 103.47]	**Mrr**	**-0.80**	
Depth	10 km	**Mtt**	**1.95**	
		Mpp	**-1.15**	
		Mrt	**0.08**	
Time	2:54:36.9	**Mrp**	**-0.27**	
		Mtp	**0.52**	
14 May 2008 CMT (Mw 5.5)				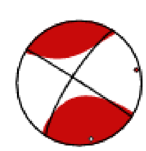
Epicenter	[31.32, 103.60]	**Mrr**	**-0.47**	
Depth	12 km	**Mtt**	**1.92**	
		Mpp	**-1.45**	
		Mrt	**-0.46**	
Time	2:54:36.9	**Mrp**	**0.04**	
		Mtp	**0.76**	

17 May 2008 CTBTO (4761579 Mw 5.9)				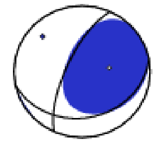
Epicenter	[32.42, 105.08]	**Mrr**	**4.01**	
Depth	10 km	**Mtt**	**-3.10**	
		Mpp	**-0.91**	
		Mrt	**-0.38**	
Time	17:08:31.5	**Mrp**	**-4.96**	
		Mtp	**-2.03**	
17 May 2008 CMT (Mw 5.7)				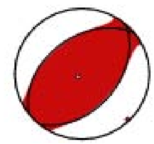
Epicenter	[32.23, 105.10]	**Mrr**	**4.76**	
Depth	14 km	**Mtt**	**-2.46**	
		Mpp	**-2.29**	
		Mrt	**-0.19**	
Time	17:08:29.7	**Mrp**	**0.45**	
		Mtp	**-2.92**	
19 May 2008 CTBTO (4765811 Mw 5.5)				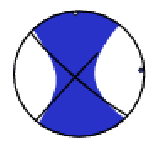
Epicenter	[32.97, 105.37]	**Mrr**	**.43**	
Depth	40 km	**Mtt**	**1.74**	
		Mpp	**-2.17**	
		Mrt	**0.08**	
Time	6:06:59.5	**Mrp**	**0.24**	
		Mtp	**0.22**	
25 May 2008 CTBTO (4770155 Mw 5.9)				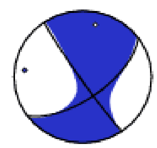
Epicenter	[32.69, 105.43]	**Mrr**	**1.3**	
Depth	10 km	**Mtt**	**6.44**	
		Mpp	**-7.74**	
		Mrt	**1.78**	
Time	8:21:51.8	**Mrp**	**-3.10**	
		Mtp	**-2.31**	
25 May 2008 CMT (Mw 6.0)				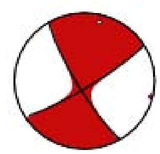
Epicenter	[32.60, 105.48]	**Mrr**	**1.13**	
Depth	15 km	**Mtt**	**11.30**	
		Mpp	**-12.40**	
		Mrt	**2.61**	
Time	8:21:53.0	**Mrp**	**-0.47**	
		Mtp	**-6.22**	
27 May 2008 CTBTO (4769576 Mw 5.45)				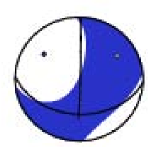
Epicenter	[32.80, 105.66]	**Mrr**	**0.05**	
Depth	10 km	**Mtt**	**0.12**	
		Mpp	**-0.17**	
		Mrt	**-0.45**	
Time	8:37:55.7	**Mrp**	**-1.03**	
		Mtp	**-0.95**	
27 May 2008 CMT (Mw 5.5)				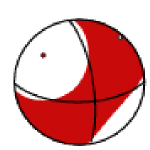
Epicenter	[32.75, 105.71]	**Mrr**	**-0.02**	
Depth	15 km	**Mtt**	**0.37**	
		Mpp	**-0.36**	
		Mrt	**-0.87**	
Time	8:37:55.2	**Mrp**	**-1.26**	
		Mtp	**-1.60**	

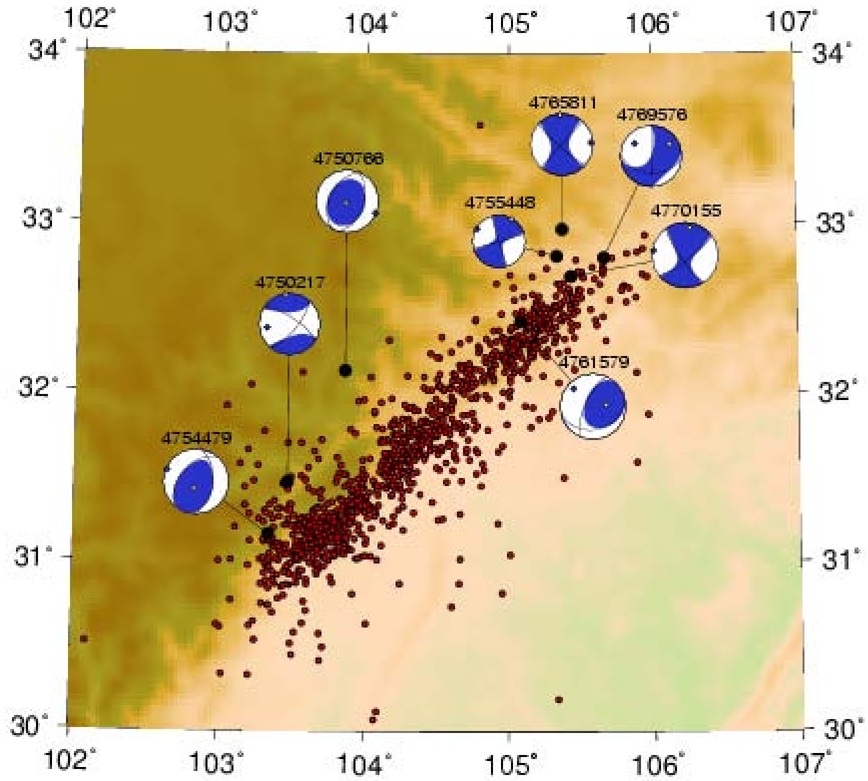

Figure 1. This figure shows the locations (small red dots) of the May 12 2008, Sichuan aftershocks from 12 May to 3 June in the Reviewed Events Bulletin from the CTBTO IDC. The total number of aftershocks shown in the figure is 1,088. Also shown are the centroid locations (larger black dots) and the MTs for eight of the aftershocks (see Table 1) for which we have a surface-wave MT inversion result. The specifications of each of the MTs shown on this figure are listed in Table 1. To link the events presented in the figure to Table 1, refer to the unique number (orid number) on top of each focal mechanism.

CONCLUSIONS AND RECOMMENDATIONS

We have developed and integrated surface-waves MT inversion software into the IDC processing environment on an experimental basis. The inversion is integrated into a Web page where the user can toggle between several databases including an experimental database containing fast bulletins with events that occurred in the past 20 minutes, and the IDC archive database. At present, an experienced user can obtain a fast MT with a few mouse clicks and within a few minutes for events in these databases.

We are presently evaluating the method and the dispersion models used in the inversion. It is clear from the initial results that the method is routinely applicable to some events of magnitudes as low as 4.5 when it is possible to extract the frequency-amplitude information from the waveforms.

ACKNOWLEDGEMENTS

We thank Drs. Lassina Zerbo, IDC Director, and Jack Shlachter, IDC Coordinator, for allowing us to publish this research and for their support.

REFERENCES

Abe, K., (1995), Magnitudes and Moments of Earthquakes, in Global Earth Physics, A Handbook of Physical, AGU Reference Shelf 1:206, 213.

Ekström, G. , J. Tromp, and E.W.F. Larson (1997). Measurements and global models of surface wave propagation, *J. Geophys. Res.* 102: (B4), 8137–8157.

Hanks T.C. and H. Kanamori (1979). A moment magnitude scale. Journal of Geophysical Research 84 (B5): 2348–50.

Stevens, J. L., D. A. Adams, G. E. Baker, M. G. Eneva and H. Xu (2005), "Improved Surface Wave Dispersion Models, Amplitude Measurements and Azimuth Estimates," SAIC Final Report submitted to AFRL under contract DTRA01-01-C-0082, March

Disclaimer